Performance comparison of induction motor and line start PM motor for cooling fan applications (repository copy)

Article:

Mutize, C., Wang, R-J., (2013) Performance comparison of induction motor and line start PM motor for cooling fan applications, *Proc. of the Southern African Universities Power Engineering Conference*, (SAUPEC), North-West University, Potchefstroom, South Africa, pp. 122--126, 31 January - 1 February 2013

PERFORMANCE COMPARISON OF INDUCTION MOTOR AND LINE START PM MOTOR FOR COOLING FAN APPLICATIONS

C. Mutize and R-J. Wang*

* *Department of Electrical and Electronic Engineering, Stellenbosch University, Private Bag X1, Matieland 7602, South Africa E-mail: mutizec@gmail.com; rwang@sun.ac.za*

Abstract: This paper presents the design of a line-start permanent magnet (LSPM) motor by modifying a commercial premium efficiency cage induction motor (IM) for cooling fan applications. Two-dimensional transient finite element (FE) analysis is applied to both IM and LSPM motor to compare their starting and synchronization performance for fan-type load. It clearly shows that the LSPM motor has better efficiency and power factor than that of IM at steady-state. However, the transient starting performance of the LSPM compares less favorably with that of the IM.

Key words: Line-start motor, permanent magnet, induction motor, design optimisation, finite element method, transient performance, cage winding.

1. INTRODUCTION

Line-start motors are usually squirrel-cage induction motors, which are of relatively poor efficiency, power factor and power density. Global environmental concerns raise the need for improving energy efficiency in industry. There has been significant research effort into developing alternative energy efficient motors. Amongst others, the line-start permanent magnet (LSPM) synchronous motor has been regarded as a promising candidate to replace traditional line-start induction motor. The difference between LSPM synchronous motor and adjustable speed PM synchronous motor is that the former has cage winding in the rotor to assist with starting. The concept of LSPM synchronous motor was first described by Binns in 1971 [1]. Comparing with induction motor, the LSPM synchronous motor is of the following merits:

- High power factor (consume no reactive power);
- Under steady-state, there is no winding loss in rotor so that the efficiency can be high;
- Considering relatively low thermal loading, it is even possible to remove fan for small power machines;
- The air-gap in a LSPM motor is usually larger than that of induction motor, which can effectively reduce stray loss.

Although LSPM motors possess many advantages over induction motors, the design of this type of motor still has many challenges. This is mainly attributed to that LSPM motor has to fulfil both asynchronous starting and synchronous operations. With both magnets and cage wind-ing in the same rotor, there is an inherent competition of space between them, which often unavoidably leads to a quite complicated rotor structure. Furthermore, the localized magnetic saturation in various parts of the machine also makes it very difficult to accurately predict some key performance parameters especially during the transient process. In short, the rotor design of LSPM motor is not an easy task.

Although a lot of research has been done on the LSPM motor topics [1–8], the challenge remains the limited synchronisation capability with inertia. This paper compares the steady-state and transient starting and synchronisation behaviour of an induction motor with that of a LSPM motor for cooling fan applications.

1.1 Characteristics of fan-type load

The load torque is proportional to the square of the fan rotation speed. This type of loads exhibit variable load torque characteristics requiring much lower torque at low speeds than at high speeds, which implies that the load torque is relatively low when starting up.

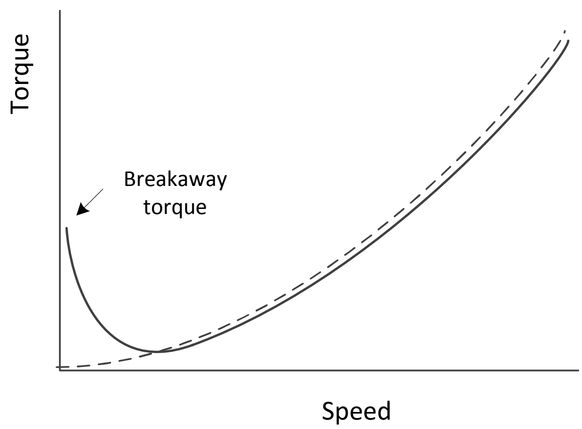

Figure 1: Torque-speed characteristics for fan-type load.

The steady-state torque-speed characteristics of fans may be represented by the shape shown in Fig. 1 (dotted line). These characteristics are often approximately represented by assuming that the torque T required is proportional to the square of the speed n:

$$T = T_{rated} \times (\frac{n}{n_{rated}})^2 \quad (1)$$

where T_{rated} and n_{rated} are rated torque and speed of a fan load respectively. Note that this approximation is generally invalid at low speeds because most practical fans have to overcome a significant breakaway torque (as shown in Fig. 1) when starting. A more practical fan torque-speed curve is thus implemented in the transient analysis.

2. INDUCTION MOTOR CONFIGURATION

A WEG 2.2kW 525V 4-pole three-phase premium efficiency cage induction motor has been selected as a reference motor for the study. The winding layout of the induction motor under study is given in Fig. 2. From a production perspective, it would be cost-effective if standard IMs can be easily modified to a LSPM motor. In this study, the stator and rotor cage winding is kept unchanged.

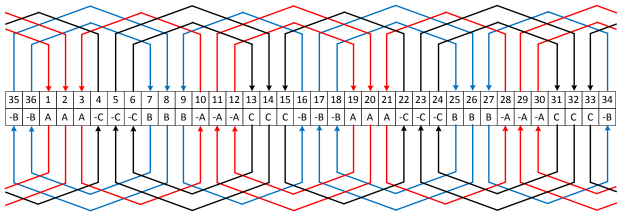

Figure 2: The winding layout of the induction motor stator.

3. DESIGN OF LINE-START PM MOTOR

The design of a LSPM motor can be a complicated multi-variable and multi-criteria optimization problem [6]. Since the same stator and cage winding are used, the only variables are those that change the magnet position, size of magnets and the width of the rib as shown in Fig. 3.

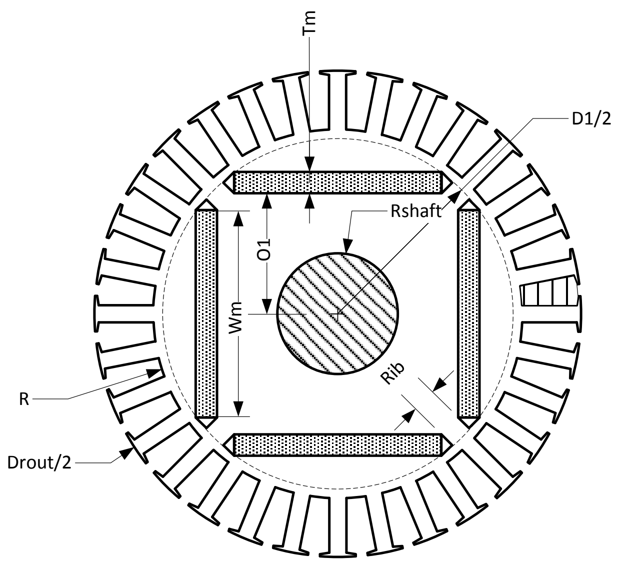

Figure 3: The selected LSPM topology.

3.1 Design optimization

The basic design method employed here is to use a combination of both analytical and FEM performance calculations. Considering the less demanding starting torque requirement of fan-type loads, the design optimisation is performed for steady-state and full-load condition by using analytical method. The objective is to optimise for maximum efficiency while subjected to the constraints such as output power and power factor.

Table 1: Main design dimensions of LSPM.

Description	Stator	Rotor
Outer diameter (mm)	160	97.9
Inner diameter (mm)	99.9	26.8
Axial length (mm)	121	121
Wire diameter (mm)	0.643	-
Winding type	lap	cage
Coil pitch	23/3	-
Phase connection	Delta	-
Number of slots	36	28
Number of conductors per slot	82	-
Number of strands per conductor	2	-
Magnet width (mm)	-	32.96
Magnet thickness (mm)	-	5.68
Air-gap length (mm)	1	-

The generated optimum design is then verified by using 2D transient FE analysis to check the starting and synchronization performance. In the case that the motor fails to start, new design iterations need to be carried out until a satisfactory design is found. The flow chart of the LSPM motor design procedure is given in Fig. 4. The main dimensions of the optimum design of LSPM motor are summarised in Table 1.

4. PERFORMANCE COMPARISON

To compare the performance of LSPM motor with that of IM for cooling fan applications, both steady-state and transient performances of both type motors are simulated and presented in the following subsections.

4.1 Steady state

As shown in Fig. 5, it can be observed that the LSPM draws lower current than that of induction motor at steady-state. The induced voltages (EMF) (Fig. 6) for both motors are practically the same, which implies that the amount of magnet material used is appropriate. The comparison of the steady-state performance of IM and LSPM motors is given in Table 2. It is evident that LSPM motor has better efficiency and power factor than that of IM.

4.2 Transient performance

The transient performance of LSPM motor is of particular interest as this type motor is known for its relatively poor transient performance. Transient 2D FE analysis has been applied to calculate the starting and synchronization performances. For both motors the stator is powered from 3-phase 525V supply at 50Hz frequency. The system inertia and fan-load characteristic have also been

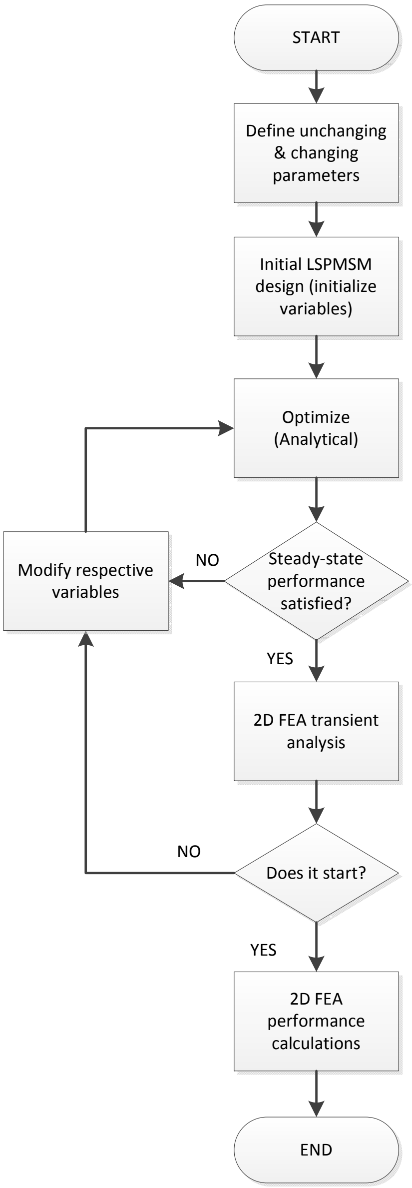

Figure 4: Flow chart of LSPM motor design procedure.

implemented in the FE analysis. For a load torque of T_L, the instantaneous rotor acceleration is governed by the following equation:

$$\frac{d\omega_r}{dt} = \frac{P}{J}(T_e - T_L) \quad (2)$$

where T_e is the electromagnetic torque, J is the inertia, P is the number of pole pairs, ω_r is the angular speed of the rotor. Fig. 8 is the flux plot of the LSPM motor under full load at a certain time step.

Figs 8-9 show the current waveforms of both motors during load starting process. It can be seen that LSPM motor draws slightly higher starting current than that of IM.

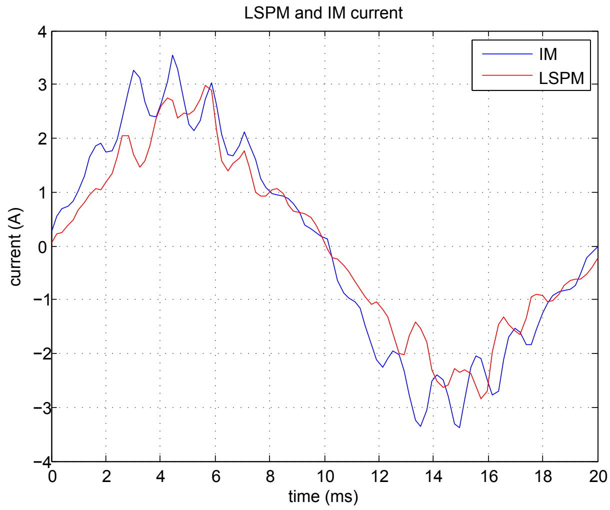

Figure 5: Steady-state currents of IM and LSPM.

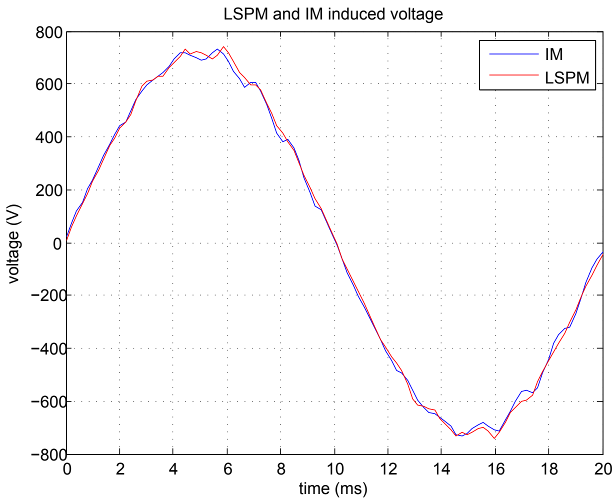

Figure 6: Induced voltages of IM and LSPM.

The speed-time responses for both LSPM motor and induction motor under load are plotted on the same graph as shown in Fig. 10. The IM is pulled into synchronism about 80 ms faster than that of LSPM motor. Figs 11-12 show the torque-time characteristics for both motors at the same condition.

As shown in Figs 13-14, for fan-type loads with relatively low inertia, the instantaneous speed-torque trajectory for both LSPM motor and induction motor show no sign of repetitive pole-slips profiles at starting. The synchronization process for both motors are satisfactory, though the IM demonstrates a slightly better performance with a smaller locus surrounding rated speed.

5. CONCLUSION

This paper presents the design of a LSPM motor by simply modifying a commercial premium efficiency IM for cooling fan applications. The steady-state and transient

Table 2: Steady state performance of IM and LSPM.

Description	LSPM	IM
Power (kW)	2.28	2.22
Current (A)	2.5	3.47
Voltage (V)	525	525
Rated speed (rpm)	1500	1435
Efficiency (%)	93.6	87
Power factor	0.99	0.8
Rated torque (Nm)	14	14.6
Frame size	100L	100L

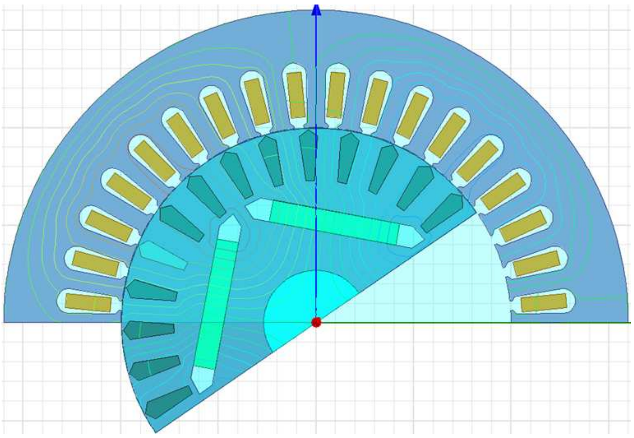

Figure 7: Flux plot of the LSPM under full load.

performances of both motors are computed and compared by applying extensive 2-D transient FE analysis. It clearly shows that the LSPM motor has better efficiency and power factor than that of IM at steady-state. Although the excellent transient starting performance of the LSPM is evident, the IM exhibits a slightly better overall transient performance for fan-type loads.

ACKNOWLEDGMENT

This work was supported in part by Eskom Tertiary Education Support Program (TESP), Sasol Technology Research and Development, and the National Research Foundation (NRF).

REFERENCES

[1] T.J.E. Miller: "Synchronization of line-start permanent magnet ac motors", *IEEE Trans. PAS* 103:1822-1828, 1984.

[2] W. Fei, P. Luk, J. Ma, J. Shen and G. Yang: "A high performance line-start permanent magnet synchro-nous motor amended from a small industrial three-phase induction motor", *IEEE Trans Magnetics*, vol.45, no.10, pp.4724-4727, October 2009.

[3] J. Li, J. Song and Y. Cho: "High performance line start permanent magnet synchronous motor for pumping system", *2010 IEEE International Symposium on Industrial Electronics (ISIE)*, pp.1308-1313, 4-7 July 2010.

[4] T. Ding, N. Takorabet, F. Sargos, X. Wang: "Design and analysis of different line-start PM synchronous motor for oil-pump applications", *IEEE Trans Magnetics*, vol.45, no.3, pp.1816-1819, March 2009.

[5] A. Isfahani, S. Vaez-Zadeh, A. Raham: "Evaluation of synchronization capability in line start permanent magnet synchronous motors", *IEEE International Electric Machines and Drives Conference (IEMDC)*, pp.1346-1350, 2011.

[6] W. Jazdzynski, M. Bajek: "Modeling and bi-criterial optimization of a line start permanent magnet synchronous machine to find an IE4 class high efficiency motor", *International Conference on Electrical Machines (ICEM)*, 6p, September 2010.

[7] A. Aliabad, M. Mirsalim, N. Ershad: "Line-start permanent magnet motors: significant improvements in starting torque, synchronization, and steady-state performance", *IEEE Trans Magnetics*, vol.46, no.12, pp.4066-4072, December 2010.

[8] W. Kim, K. Kim, S. Kim, D. Kang, S. Go, H, Lee, Y. Chun, J. Lee: "A study on the optimal rotor design of LSPM considering the starting torque and efficiency", *IEEE Trans Magnetics*, vol.45, no.3, March 2009.

APPENDIX

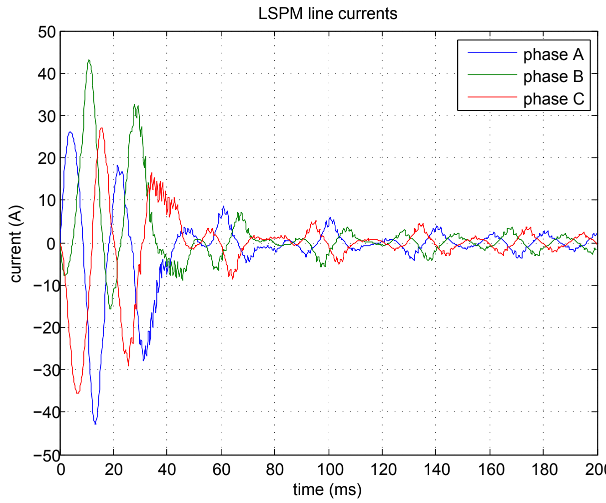

Figure 8: LSPM line currents versus time (under load).

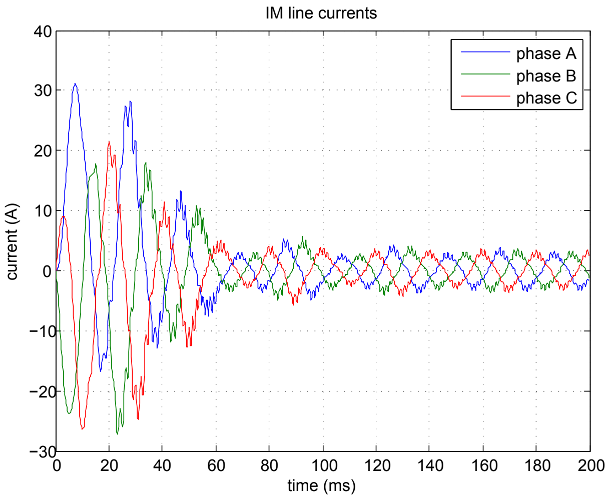

Figure 9: IM line currents versus time (under load).

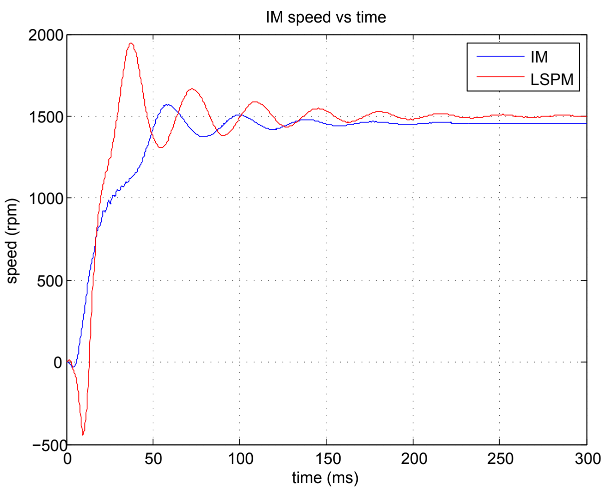

Figure 10: Speed versus time curves of LSPM and IM

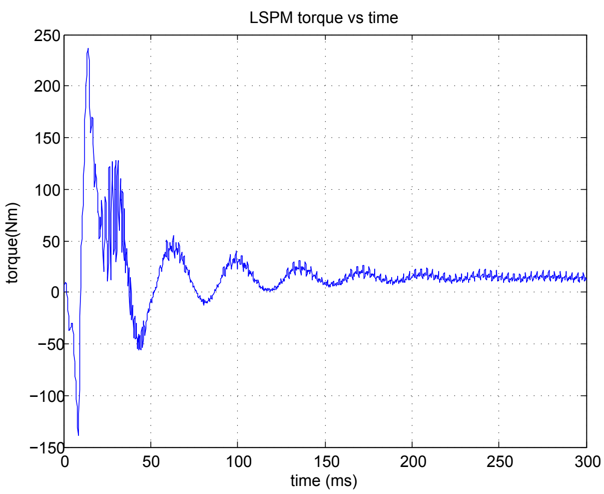

Figure 11: LSPM torque versus time (under load).

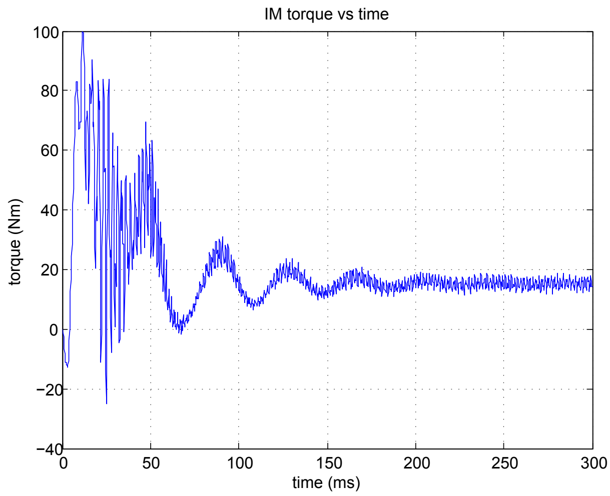

Figure 12: IM torque versus time (under load).

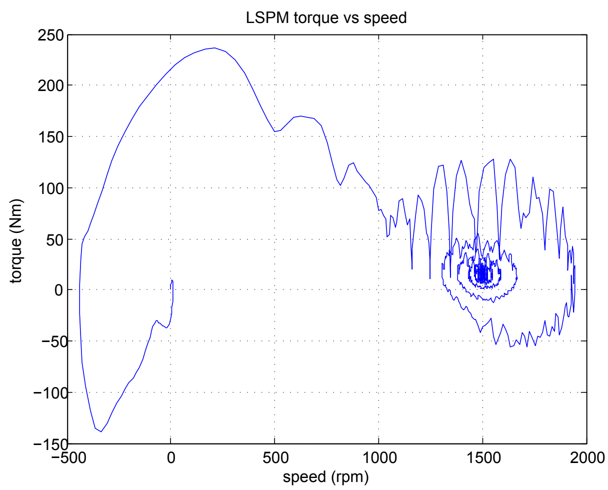

Figure 13: LSPM transient torque-speed trajectories.

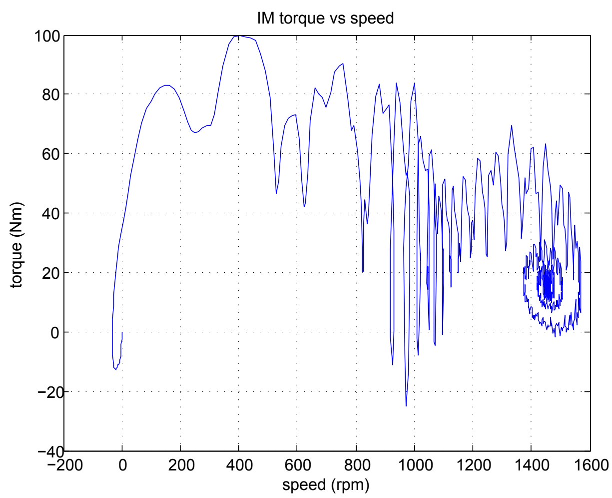

Figure 14: IM transient torque-speed trajectories.